



Published in final edited form as:

Nature. ; 483(7389): 295–301. doi:10.1038/nature10799.

## Genome-wide structure and organization of eukaryotic pre-initiation complexes

Ho Sung Rhee<sup>1</sup> and B. Franklin Pugh<sup>1</sup>

<sup>1</sup>Center for Eukaryotic Gene Regulation, Department of Biochemistry and Molecular Biology, The Pennsylvania State University, University Park, Pennsylvania 16802, USA

### SUMMARY

The structural and positional organization of transcription pre-initiation complexes (PICs) across eukaryotic genomes is unknown. We employed ChIP-exo to precisely examine ~6,000 PICs in *Saccharomyces*. PICs, including RNA polymerase II and general factors TFIIA, -B, -D/TBP, -E, -F, -H, and -K were positioned within promoters and excluded from coding regions. Exonuclease patterns agreed with crystallographic models of the PIC, and were sufficiently precise to identify TATA-like elements at so-called TATA-less promoters. These PICs and their transcription start sites were positionally constrained at TFIID-engaged +1 nucleosomes. At TATA box-containing promoters, which are depleted of TFIID, a +1 nucleosome was positioned to be in competition with the PIC, which may afford greater latitude in start site selection. Our genomic localization of mRNA and noncoding RNA PICs reveal that two PICs, in inverted orientation, may occupy the flanking borders of nucleosome-free regions. Their unambiguous detection may help distinguish bona-fide genes from transcriptional noise.

### Keywords

GTFs; TAFs; *Saccharomyces*; ChIP-seq; transcription initiation

Assembly of the PIC and its post-assembly control are critical early steps in transcription of eukaryotic genes. TBP (TATA-binding protein) arrives at most promoters as part of the multisubunit TFIID complex that includes TBP-associated factors (TAFs)<sup>1</sup>. Together these proteins help recruit RNA polymerase (pol) II and its entourage of general transcription factors (GTFs) to the transcription start sites (TSS) of genes<sup>2-4</sup>. These PICs assemble in nucleosome-free promoter regions (NFRs) that are flanked by an upstream -1 nucleosome and a downstream +1 nucleosome<sup>5</sup>. PICs have largely been defined biochemically using

Users may view, print, copy, download and text and data- mine the content in such documents, for the purposes of academic research, subject always to the full Conditions of use: [http://www.nature.com/authors/editorial\\_policies/license.html#terms](http://www.nature.com/authors/editorial_policies/license.html#terms)

Correspondence and requests for materials should be addressed to B.F.P (bfp2@psu.edu)..

Sequencing data has been deposited at NCBI Sequence Read Archive under accession number SRA046523. Reprints and permissions information is available at [www.nature.com/reprints](http://www.nature.com/reprints). The authors declare no competing financial interests. Readers are welcome to comment on the online version of this article at [www.nature.com/nature](http://www.nature.com/nature).

**Author Contributions** HSR performed the experiments and conducted data analyses. HSR and BFP conceived of the experiments, analyses, and co-wrote the manuscript.

**Supplementary Information** is linked to the online version of the paper at [www.nature.com/nature](http://www.nature.com/nature).

purified GTFs at a few model genes<sup>2-4</sup>, but little is known about their assembly and organization *in vivo*, particularly at near bp resolution on a genome-wide scale.

An oddity of TBP is that when it is part of the TFIID complex, it tends to bind promoters that lack the TATA box consensus TATAWAWR (W=A/T, R=A/G)<sup>6</sup>. Approximately 80-90% of all *Saccharomyces* genes are thus designated as “TATA-less”, and have a predominant PIC assembly mechanism and chromatin architecture that differs substantially from those in the “TATA box” class of genes<sup>6-9</sup>. To date, no TBP binding motif has been identified at TATA-less promoters, and so the origins of TFIID-promoter specificity have been rather enigmatic<sup>10</sup>. When TBP is not part of the TFIID complex, the SAGA complex directs TBP to TATA box-containing pol II promoters<sup>11-13</sup>.

TFIIA and TFIIB clamp TBP to DNA, and make DNA contacts immediately upstream and downstream of the TATA box. TFIIB is a linchpin between TBP and pol II<sup>14,15</sup>. Its intimate contact with pol II directs how far downstream pol II productively initiates transcription<sup>16,17</sup>. TFIIF enhances the interaction of pol II with TFIIB, assists in recruiting TFIIE, and promotes downstream elongation events<sup>3,18</sup>. TFIIE then stimulates DNA strand separation by pol II at the transcription start site (TSS), and enhances the activity of TFIIH. TFIIH holoenzyme is multi-functional, having ATP-dependent helicase (Ssl2 and Rad3) and kinase (Kin28) activities that reside on biochemically separable sub-complexes (TFIIH and TFIIK, respectively), both of which are key to efficient open complex formation and transcription initiation<sup>19-21</sup>.

We examined the structural organization of PICs and their specificity on a genomic scale by applying lambda exonuclease to chromatin immunoprecipitates (termed CHIP-exo)<sup>22</sup>. This novel strategy substantially improved mapping resolution and eliminated many false positives. The exonuclease processively degrades a DNA strand in the 5'-3' direction until a crosslinking point is encountered (Supplementary Fig. 1a). The crosslinking inefficiency inherent to ChIP allows multiple crosslinking points to be detected in a population by deep sequencing. When applied to the GTFs on a genomic scale, we obtained detailed and comprehensive information on PIC structure and genomic organization.

## Genome-wide PIC structure

We applied CHIP-exo genome-wide to pol II and each GTF (Fig. 1a), and verified binding for TFIIB by locus-specific PCR using a series of tiled primers (Supplementary Fig. 1b). When exonuclease stop sites were mapped over all annotated mRNA promoters that contained a TATA box consensus, a distinctive pattern was observed (Fig. 1b). Importantly, each GTF displayed a strand-specific composite pattern of exonuclease stop sites that occurred only when TATA boxes, but not TSSs (Supplementary Fig. 2a and data not shown), were aligned, indicating that PICs are positioned with respect to the TATA box.

For TFIIB, we detected four DNA crosslinking points (pairs of exonuclease stops), designated B1-B4 (Fig. 1c). The TATA box was precisely centered between B1 and B2, which were separated by  $20 \pm 3$  bp. Crosslinking point B3 and the diffuse B4 region indicate that TFIIB further crosslinked over a broad region downstream of the TATA box towards the TSS. We compared the four TFIIB crosslinking points to crystallographic-based models

of “open” and “closed” TBP/TFIIB/pol II/promoter complexes (Fig. 1c)<sup>14,15</sup>. An important caveat of the crystallographic models is they were built from multiple independent structures of truncated TFIIB•TBP•TATA, TFIIB•pol II, and pol II elongation complexes. Thus, the combined structures represent a hypothetical organization.

Within the modeled closed and open structures, crosslinking site B1 precisely ( $\pm 3$  bp) mapped to where the TFIIB C-terminal core straddles the upstream DNA-binding stirrup of TBP (11 bp upstream of the TATA box midpoint). B2 mapped precisely ( $\pm 3$  bp) to where the TFIIB core N-terminal cyclin fold encounters DNA just downstream of TBP’s other stirrup (9 bp downstream of the TATA box midpoint). B3 mapped to where the TFIIB “linker” region is closest to DNA, which was 19 bp downstream of the TATA box midpoint. B4 corresponded to a broad region defined by close proximity of TFIIB “reader”/“finger” to single-stranded DNA within the modeled open complex, but was not evident within the closed complex. Similar broad regions of crosslinking were observed with the other GTFs (Fig. 1b), and may reflect indirect crosslinking. Support that these PICs represent open complexes is provided by permanganate reactivity studies of the *GALI-10* and *HSP82* loci<sup>23,24</sup>. Taken together, the entirety of the genomic crosslinking sites observed with the GTFs and pol II fits remarkably well with the crystallographic models of the PIC open complex<sup>14,15</sup>, and with many aspects of *in vitro* chemical crosslinking of these proteins<sup>19,25-27</sup>.

### TATA-like elements at “TATA-less” genes

An apparent paradox of so-called “TATA-less” promoters is their utilization of TFIID, which has long been described as the TATA box-binding complex<sup>4</sup>. Does the TBP subunit of TFIID recognize specific DNA sequences at TATA-less promoters? Inasmuch as TBP is expected to be found at all TATA-less promoters, and motif searching algorithms failed to identify candidate TBP binding sites, we instead opted to search for sequence elements with up to two mismatches to the TATAWAWR consensus. We also limited our search to measured PIC locations. Remarkably, 99% of the PICs at TATA-less promoters contained a sequence having two or less mismatches to the TATA box consensus (Fig. 2). We refer to these mismatched elements as “TATA-like”, as they did not form a consensus, whereas those conforming to the consensus retain the “TATA box” designation. We refer to the two elements together as “TATA elements”.

To assess whether TFIIB was positioned around these TATA-like elements in a canonical manner as seen at bona-fide TATA boxes, strand-specific ChIP-exo tags were plotted around each element, separated into panels by 0, 1, or 2 mismatches to the TATA box consensus (Fig. 2). Strikingly, regardless of its occupancy level, the distribution of TFIIB crosslinking and thus its positioning relative to these TATA-like elements (lower two panels) was quite similar to the positioning observed at bona-fide TATA boxes (upper panel). When the other GTFs were examined, their patterns relative to TATA-like elements were also similar to those found at TATA boxes (Supplementary Fig. 2b), although some downstream differences were observed (addressed below). Thus, as previously seen at the three yeast TATA box-containing genes *GALI, 10* and *HSP82*<sup>23,24</sup>, and in mammalian *in vitro* systems<sup>28</sup>, at least the upstream portion of most PICs are positioned with respect to

resident TATA elements nearly identically, regardless of their pol II promoter classification as TATA box-containing or TATA-less. Although the “TATA-less” designation may be a misnomer, this class of genes is not simply a slight variation of the TATA class, but instead have predominant regulation by TFIID vs SAGA, positive vs negative regulation by chromatin, and lower “plasticity” of expression<sup>6-9</sup>.

## TATA-less TSS positioning by nucleosomes

Permanganate reactivity experiments detect open complex formation upstream of the TSS at the *GALI,10* and *HSP82* TATA box-containing promoters<sup>23,24</sup>. These and other studies<sup>17,29</sup> have led to the notion that pol II scans downstream from the open complex to find the TSS. In agreement as a general mechanism, we find that PICs of TATA box-containing genes generally reside upstream of the TSS (Supplementary Fig. 2a).

TAFs are largely depleted at TATA box-containing promoters, although they are not entirely absent (Fig. 3a). The low level of TAF1 that was present tended to be positioned similarly to TBP and other GTFs (Figs. 1b, and Supplementary Fig. 2a,b). In contrast, TAF1-enriched/TATA-less promoters (which are related, as shown in Supplementary Fig. 3) revealed additional interactions downstream of the TSS that exactly coincide with the size and location to the +1 nucleosome (Fig. 3a). Indeed, TAF1 displayed a more uniform positioning pattern in relation to the TSS and +1 nucleosome than to TATA elements, which suggests that at least part of the TFIID TAF complex engages and is positioned by the +1 nucleosome at TATA-less promoters. Consistent with this, Bdf1, which is considered to be a missing piece of TAF1<sup>30</sup>, binds to the +1 nucleosome<sup>31</sup>. Furthermore, Bdf1 showed a nearly identical CHIP-exo pattern as TAF1 (Supplementary Fig. 4). TFIID-nucleosomal interactions have also been reported in mammalian systems, although the details may differ<sup>32</sup>.

If TFIID binds simultaneously to both the +1 nucleosome and a TATA element, then the intervening pol II would seem to be fenced in by TFIID, thereby limiting its ability to scan DNA. This model predicts that the TSS would reside closer to the TATA element and be positionally restricted relative to the +1 nucleosome, compared to TAF1-depleted/TATA box-containing promoters. Indeed, the TSS at TATA-less promoters resided ~10-20 bp closer to the TATA element than at TATA box-containing promoters (Supplementary Fig. 2a).

We also compared the position of TATA elements and TSSs in relation to the +1 nucleosome. We separately examined individual TAF1-depleted/TATA-box containing and TAF1-enriched/TATA-less promoters (Fig. 3b). Strikingly, at the TAF1-enriched promoters (lower panel), the TSS was tightly positioned at the border between the 5' NFR and the +1 nucleosome in comparison to TAF1-depleted/TATA-box containing promoters. The latter had TSSs distributed across the adjacent nucleosome position, and these nucleosomes were relatively depleted compared to the TAF1-enriched class (Fig. 3a).

Taken together, we interpret these observations to reflect distinct functions of the +1 nucleosome at the two classes of genes. Nucleosomes and PICs might cooperatively assemble at the TFIID-enriched/TATA-less class, where the nucleosome may be instructive for TSS selection by impeding pol II scanning. In contrast, nucleosomes and PICs may

competitively assemble at the TAF1-depleted/TATA box-containing class. This may allow for greater stochasticity or plasticity of expression that is characteristic of this class<sup>9</sup>, where nucleosome loss would prime the gene for a high level of transcription. A nucleosome competition mechanism removes an impediment to pol II scanning. Pol II could scan further, thereby allowing productive initiation at specific DNA elements<sup>33</sup>. The transition into a scanning state may be rate-limiting in the scanning cycle since the PIC is detected upstream of the TSS.

## GTF depletion in genes and their termini

While it is clear that GTFs assemble in promoter regions of mRNA genes and disengage pol II within ~150 bp of the TSS<sup>34-37</sup>, it is less clear as to the extent to which they assemble across the body of genes, or at genes that are either transcriptionally silent or classified as “dubious”. A whole genome view of GTFs and pol II is presented in Fig. 4a. Remarkably, PICs were almost entirely excluded from coding regions, regardless of gene activity, whereas pol II was enriched across gene bodies as expected. Approximately 90% of “dubious” ORFs lacked a canonical PIC organization or contained PICs within the ORF, and thus are unlikely to be coding. Thus, coding region PIC-driven initiation whether in the sense or anti-sense direction is infrequent on the scale of what is seen at mRNA promoters. Moreover, the observed GTF pattern makes clear that pol II disengages all GTFs at the promoter.

Much less is known of the fate of pol II at the ends of genes, as it undergoes termination. To examine the 3' ends of genes, without complications associated with nearby mRNA promoters, we separated 3' ends into those having nearby 3' or 5' ends of an adjacent gene (Fig. 4b). Within terminal intergenic regions, GTFs were highly depleted, indicating that PICs rarely exist at the 3' ends of genes at levels seen for mRNA genes (although lower levels do exist).

Remarkably, we find a highly correlated enrichment of pol II and TFIIH (Ssl2) but not TFIK (Kin28), at the end of genes within 3' NFRs (Fig. 4b). Such a physical separation of the TFIH/Ssl2 and TFIK/Kin28 submodules of holo-TFIH in genome-wide binding experiments has not previously been reported, but may be in accord with their biochemistry<sup>19-21</sup>. However, Ssl2 is biochemically separable from the TFIH core, which therefore prompted us to examine additional core TFIH subunits, Ssl1 and Tfb1. Surprisingly, both were absent from the ends of genes (Supplementary Fig. 6), although present within PICs at promoters. These results suggest that Ssl2, a 3'-5' helicase, operates independently of holo-TFIH at the ends of genes. Consistent with a possible role of Ssl2 in transcription termination, Ssl2 has functional interactions with the Hsp90 protein chaperone<sup>40</sup>, which has been implicated in the disassembly of the transcription machinery<sup>41</sup>.

## Divergent transcription from distinct PICs

In contrast to coding regions, PICs were abundant in intergenic regions, far beyond what could be accounted for at mRNA promoters (Fig. 4c). Divergent transcription, where mRNA and ncRNA initiation occurs within the same region but elongates in opposite directions, is well established in eukaryotes<sup>42,43</sup>. However, it has been unclear whether divergent

transcription originates from the same PIC site. Conceivably, the entire PIC or a portion thereof might assemble in either direction. As shown in Fig. 4c, even the shortest (~120 bp) 5' intergenic regions of mRNA genes with inverted orientation were associated with two PICs, one for each mRNA direction. Thus, divergent mRNA transcription originates from two distinct PICs, even when arising from the same NFR.

We next examined the composition and location of PICs associated with mRNA and ncRNA (variously classified as CUTs, SUTs, XUTs, and Antisense (AS))<sup>44-46</sup>. We also examined “orphan” PICs which we defined as being >160 bp from any annotated TSS or ORF start site. Nearly all had the same relative composition of GTFs, including TAF1 depletion or enrichment (Fig. 5a), albeit mRNA PICs generally had higher occupancy levels. GTFs had highly correlated occupancies at all PICs (see Supplementary Fig. 7 for mRNA PICs). ncRNA PICs were generally organized around an adjacent nucleosome as seen for mRNA PICs (Supplementary Fig. 8). Thus, all mRNA, ncRNA, and orphan PICs are compositionally homogeneous with regards to the GTFs (excluding TAFs).

To better visualize the context of the low-occupancy ncRNA PICs with mRNA genes, we marked ncRNA PIC locations by their TATA element, and plotted their directionality with respect to nearby mRNA (Fig. 5b). We observed a general trend where ncRNA and mRNA PICs were positioned in opposite directions 150-200 bp apart. This places both PICs within the same NFR, and thus within the same canonical nucleosome architecture as seen for two divergent mRNA PICs that share the same NFR (Supplementary Fig. 9).

Low occupancy ncRNA PICs were also found towards the 3' ends of mRNA genes, of which the majority were antisense to the mRNA (Fig. 5b), and associated with low expression of the sense mRNA (Supplementary Fig. 10a). Thus, ncRNAs, which tend to be antisense<sup>42</sup>, are generally associated with repression when residing in gene bodies.

In total, we identified ~6,000 PICs in rapidly growing yeast cells, in which the PICs had an occupancy level of >10% of the genome average. >98% of these PICs had a TATA element precisely where TBP bound. Approximately 70% of the identified PICs were associated with mRNA genes (Supplementary Fig. 10b). The remaining ~30% were divided evenly between ncRNA and orphans. At lower detection thresholds, many more low-occupancy PICs could be identified. We do not believe that they represent technical noise, since they are highly enriched in NFRs where mRNA and ncRNA PICs are found. They might produce low levels of promoter-specific basal transcription.

## Unifying principles of PICs

Our data suggest that with the exception of TAFs, PICs are compositionally homogeneous in regards to GTFs at coding and noncoding pol II transcription units in the yeast genome. PICs differ markedly in occupancy levels, which is in accord with their transcription frequency. PICs tend to form at NFR/nucleosome borders at the 5' end (and to some extent at the 3' end) of genes, where they direct either mRNA or ncRNA transcription away from the NFR. As such, an NFR may normally accommodate two divergently-oriented PICs at markedly different occupancy and transcription levels. These occupancy levels do not strictly correlate, which suggests largely independent control of the two PICs.



PIC assembly, orientation, and positioning may be contributed in part by the resident TATA element, as well as through sequence-specific factors and co-factors. TFIID-regulated promoters may rely less on TATA element strength, and rely more on an NFR-adjacent nucleosome for PIC assembly, orientation, and positioning. The adjacent nucleosome might also serve to impede a scanning pol II so that it might productively select a TSS at a focused position just inside the nucleosome. At SAGA-regulated promoters, which tend to contain a consensus TATA box, nucleosome occupancy may be more competitive with PIC assembly, wherein the strength of TBP/TATA interactions would be more important for PIC assembly, orientation, and positioning. As such, there would be no nearby nucleosome to impede polymerase scanning, which would allow TSS selection to be controlled by other factors including DNA sequence.

The emergent concept of ncRNA and the difficulty of distinguishing random transcriptional noise from specific initiation raise the question as to what constitutes a gene<sup>47</sup>. The unambiguous and precise mapping of PIC locations across a genome, as described here, might help define the start of individual genes.

## METHODS

*Saccharomyces* strains (BY4741) bearing TAP-tagged GTF or pol II subunits (or untagged TBP) were grown to exponential phase in YPD media (30°C to OD = 0.8), then subjected to 1% formaldehyde crosslinking for 15 min at 25°C. Cells were harvested and washed. Sonicated chromatin was prepared by standard methods. Standard ChIP methods were employed, followed by lambda exonuclease treatment and library construction as described elsewhere<sup>22</sup>. Libraries were sequenced by an ABI SOLiD sequencer. Figures displaying strand-specific sequencing tags represent the raw data without normalization to input. TFIIB peak calls were made with GeneTrack software<sup>48</sup>. PICs (n = 6,045) were identified as having a TFIIB peak-pair in at least two out of four biological replicates and having  $\geq 3$  sequence tags (> 10% of average TFIIB occupancy)<sup>22</sup>. PICs were assigned to the nearest TSS within  $\pm 200$  bp, with mRNA<sup>49</sup> having precedence over ncRNA. For this purpose, ORFs lacking a TSS (from SGD) were assigned a hypothetical TSS based upon the genome-wide consensus. PICs of ncRNA were assigned to the nearest TSS within  $\pm 200$  bp of SUTs, CUTs, ASs, and XUTs<sup>44-46</sup>, with SUTs/CUTs having precedence over AS/XUTs. To assign directionality to orphan PICs, we compared nucleosome occupancy on the lower vs higher coordinate side of TFIIB locations. If the higher coordinate had higher nucleosome occupancy it was classified as “sense”, otherwise it was “antisense”. We validated this method by applying it to mRNA PICs, and found >91% of the assignments to be correct. We searched for TATA elements between -80 to +20 bp of the midpoint of 6,045 TFIIB-bound locations on the sense strand, first by searching for the consensus TATAWAWR, then for 1 and then 2 mismatches to the consensus. TATA element closest to -28 bp of a TFIIB peak had precedence if multiple elements were found.

## Supplementary Material

Refer to Web version on PubMed Central for supplementary material.

## Acknowledgements

We thank Istvan Albert and Yunfei Li for bioinformatic support, and members of the Pugh lab and the Penn State Center for Eukaryotic Gene Regulation for valuable discussions. Sequencing was performed at the Penn State Genomics Core Facility. This work was supported by NIH grant GM059055.

## References

1. Green MR. TBP-associated factors (TAFIIIs): multiple, selective transcriptional mediators in common complexes. *Trends Biochem. Sci.* 2000; 25:59–63. [PubMed: 10664584]
2. Buratowski S, Hahn S, Guarente L, Sharp PA. Five intermediate complexes in transcription initiation by RNA polymerase II. *Cell.* 1989; 56:549–561. [PubMed: 2917366]
3. Orphanides G, Lagrange T, Reinberg D. The general transcription factors of RNA polymerase II. *Genes Dev.* 1996; 10:2657–2683. [PubMed: 8946909]
4. Roeder RG. The role of general initiation factors in transcription by RNA polymerase II. *Trends Biochem. Sci.* 1996; 21:327–335. [PubMed: 8870495]
5. Jiang C, Pugh BF. Nucleosome positioning and gene regulation: advances through genomics. *Nat. Rev. Genet.* 2009; 10:161–172. [PubMed: 19204718]
6. Basehoar AD, Zanton SJ, Pugh BF. Identification and distinct regulation of yeast TATA box-containing genes. *Cell.* 2004; 116:699–709. [PubMed: 15006352]
7. Huisinga KL, Pugh BF. A genome-wide housekeeping role for TFIID and a highly regulated stress-related role for SAGA in *Saccharomyces cerevisiae*. *Mol. Cell.* 2004; 13:573–585. [PubMed: 14992726]
8. Lee TI, et al. Redundant roles for the TFIID and SAGA complexes in global transcription. *Nature.* 2000; 405:701–704. [PubMed: 10864329]
9. Tirosh I, Barkai N. Two strategies for gene regulation by promoter nucleosomes. *Genome Res.* 2008; 18:1084–1091. [PubMed: 18448704]
10. Sugihara F, Kasahara K, Kokubo T. Highly redundant function of multiple AT-rich sequences as core promoter elements in the TATA-less RPS5 promoter of *Saccharomyces cerevisiae*. *Nucleic Acids Res.* 2011; 39:59–75. [PubMed: 20805245]
11. Mohibullah N, Hahn S. Site-specific cross-linking of TBP in vivo and in vitro reveals a direct functional interaction with the SAGA subunit Spt3. *Genes Dev.* 2008; 22:2994–3006. [PubMed: 18981477]
12. Dudley AM, Rougeulle C, Winston F. The Spt components of SAGA facilitate TBP binding to a promoter at a post-activator-binding step in vivo. *Genes Dev.* 1999; 13:2940–2945. [PubMed: 10580001]
13. Bhaumik SR, Green MR. Differential requirement of SAGA components for recruitment of TATA-box-binding protein to promoters in vivo. *Mol Cell Biol.* 2002; 22:7365–7371. [PubMed: 12370284]
14. Kostrewa D, et al. RNA polymerase II-TFIIB structure and mechanism of transcription initiation. *Nature.* 2009; 462:323–330. [PubMed: 19820686]
15. Liu X, Bushnell DA, Wang D, Calero G, Kornberg RD. Structure of an RNA polymerase II-TFIIB complex and the transcription initiation mechanism. *Science.* 2010; 327:206–209. [PubMed: 19965383]
16. Li Y, Flanagan PM, Tschochner H, Kornberg RD. RNA polymerase II initiation factor interactions and transcription start site selection. *Science.* 1994; 263:805–807. [PubMed: 8303296]
17. Pardee TS, Bangur CS, Ponticelli AS. The N-terminal region of yeast TFIIB contains two adjacent functional domains involved in stable RNA polymerase II binding and transcription start site selection. *J. Biol. Chem.* 1998; 273:17859–17864. [PubMed: 9651390]
18. Yan Q, Moreland RJ, Conaway JW, Conaway RC. Dual roles for transcription factor IIF in promoter escape by RNA polymerase II. *J. Biol. Chem.* 1999; 274:35668–35675. [PubMed: 10585446]
19. Kim TK, Ebright RH, Reinberg D. Mechanism of ATP-dependent promoter melting by transcription factor IIF. *Science.* 2000; 288:1418–1422. [PubMed: 10827951]



20. Keogh MC, Cho EJ, Podolny V, Buratowski S. Kin28 is found within TFIIF and a Kin28-Ccl1-Tfb3 trimer complex with differential sensitivities to T-loop phosphorylation. *Mol. Cell. Biol.* 2002; 22:1288–1297. [PubMed: 11839796]
21. Svejstrup JQ, Feaver WJ, Kornberg RD. Subunits of yeast RNA polymerase II transcription factor TFIIF encoded by the CCL1 gene. *J. Biol. Chem.* 1996; 271:643–645. [PubMed: 8557668]
22. Rhee HS, Pugh BF. Comprehensive genome-wide protein-DNA interactions detected at single nucleotide resolution. *Cell.* 2011; 147:1408–1419. [PubMed: 22153082]
23. Giardina C, Lis JT. DNA melting on yeast RNA polymerase II promoters. *Science.* 1993; 261:759–762. [PubMed: 8342041]
24. Giardina C, Lis JT. Dynamic protein-DNA architecture of a yeast heat shock promoter. *Mol. Cell. Biol.* 1995; 15:2737–2744. [PubMed: 7739554]
25. Forget D, Langelier MF, Therien C, Trinh V, Coulombe B. Photo-cross-linking of a purified preinitiation complex reveals central roles for the RNA polymerase II mobile clamp and TFIIE in initiation mechanisms. *Mol. Cell. Biol.* 2004; 24:1122–1131. [PubMed: 14729958]
26. Lagrange T, et al. High-resolution mapping of nucleoprotein complexes by site-specific protein-DNA photocrosslinking: organization of the human TBP-TFIIA-TFIIB-DNA quaternary complex. *Proc. Natl Acad. Sci. USA.* 1996; 93:10620–10625. [PubMed: 8855228]
27. Chen HT, Hahn S. Mapping the location of TFIIB within the RNA polymerase II transcription preinitiation complex: a model for the structure of the PIC. *Cell.* 2004; 119:169–180. [PubMed: 15479635]
28. Pal M, Ponticelli AS, Luse DS. The role of the transcription bubble and TFIIB in promoter clearance by RNA polymerase II. *Mol. Cell.* 2005; 19:101–110. [PubMed: 15989968]
29. Kuehner JN, Brow DA. Quantitative analysis of in vivo initiator selection by yeast RNA polymerase II supports a scanning model. *J. Biol. Chem.* 2006; 281:14119–14128. [PubMed: 16571719]
30. Matangkasombut O, Buratowski RM, Swilling NW, Buratowski S. Bromodomain factor 1 corresponds to a missing piece of yeast TFIID. *Genes Dev.* 2000; 14:951–962. [PubMed: 10783167]
31. Koerber RT, Rhee HS, Jiang C, Pugh BF. Interaction of transcriptional regulators with specific nucleosomes across the *Saccharomyces* genome. *Mol. Cell.* 2009; 35:889–902. [PubMed: 19782036]
32. Vermeulen M, et al. Selective anchoring of TFIID to nucleosomes by trimethylation of histone H3 lysine 4. *Cell.* 2007; 131:58–69. [PubMed: 17884155]
33. Faitar SL, Brodie SA, Ponticelli AS. Promoter-specific shifts in transcription initiation conferred by yeast TFIIB mutations are determined by the sequence in the immediate vicinity of the start sites. *Mol. Cell. Biol.* 2001; 21:4427–4440. [PubMed: 11416123]
34. Mayer A, et al. Uniform transitions of the general RNA polymerase II transcription complex. *Nat. Struct. Mol. Biol.* 2010
35. Ahn SH, Keogh MC, Buratowski S. Ctk1 promotes dissociation of basal transcription factors from elongating RNA polymerase II. *The EMBO journal.* 2009; 28:205–212. [PubMed: 19131970]
36. Hahn S. Structure and mechanism of the RNA polymerase II transcription machinery. *Nat. Struct. Mol. Biol.* 2004; 11:394–403. [PubMed: 15114340]
37. Yudkovsky N, Ranish JA, Hahn S. A transcription reinitiation intermediate that is stabilized by activator. *Nature.* 2000; 408:225–229. [PubMed: 11089979]
38. Ansari A, Hampsey M. A role for the CPF 3'-end processing machinery in RNAP II-dependent gene looping. *Genes Dev.* 2005; 19:2969–2978. [PubMed: 16319194]
39. Singh BN, Hampsey M. A transcription-independent role for TFIIB in gene looping. *Mol. Cell.* 2007; 27:806–816. [PubMed: 17803944]
40. Flom G, Weekes J, Johnson JL. Novel interaction of the Hsp90 chaperone machine with Ssl2, an essential DNA helicase in *Saccharomyces cerevisiae*. *Curr. Genet.* 2005; 47:368–380. [PubMed: 15871019]
41. Freeman BC, Yamamoto KR. Disassembly of transcriptional regulatory complexes by molecular chaperones. *Science.* 2002; 296:2232–2235. [PubMed: 12077419]

42. Jacquier A. The complex eukaryotic transcriptome: unexpected pervasive transcription and novel small RNAs. *Nat. Rev. Genet.* 2009; 10:833–844. [PubMed: 19920851]
43. Wei W, Pelechano V, Jarvelin AI, Steinmetz LM. Functional consequences of bidirectional promoters. *Trends Genet.* 2011; 27:267–276. [PubMed: 21601935]
44. Xu Z, et al. Bidirectional promoters generate pervasive transcription in yeast. *Nature.* 2009; 457:1033–1037. [PubMed: 19169243]
45. Granovskaia MV, et al. High-resolution transcription atlas of the mitotic cell cycle in budding yeast. *Genome Biol.* 2010; 11:R24. [PubMed: 20193063]
46. van Dijk EL, et al. XUTs are a class of Xrn1-sensitive antisense regulatory non-coding RNA in yeast. *Nature.* 2011; 475:114–117. [PubMed: 21697827]
47. Gerstein MB, et al. What is a gene, post-ENCODE? History and updated definition. *Genome Res.* 2007; 17:669–681. [PubMed: 17567988]
48. Albert I, Wachi S, Jiang C, Pugh BF. GeneTrack - a genomic data processing and visualization framework. *Bioinformatics.* 2008
49. David L, et al. A high-resolution map of transcription in the yeast genome. *Proc. Natl. Acad. Sci. USA.* 2006; 103:5320–5325. [PubMed: 16569694]
50. Holstege FC, et al. Dissecting the regulatory circuitry of a eukaryotic genome. *Cell.* 1998; 95:717–728. [PubMed: 9845373]

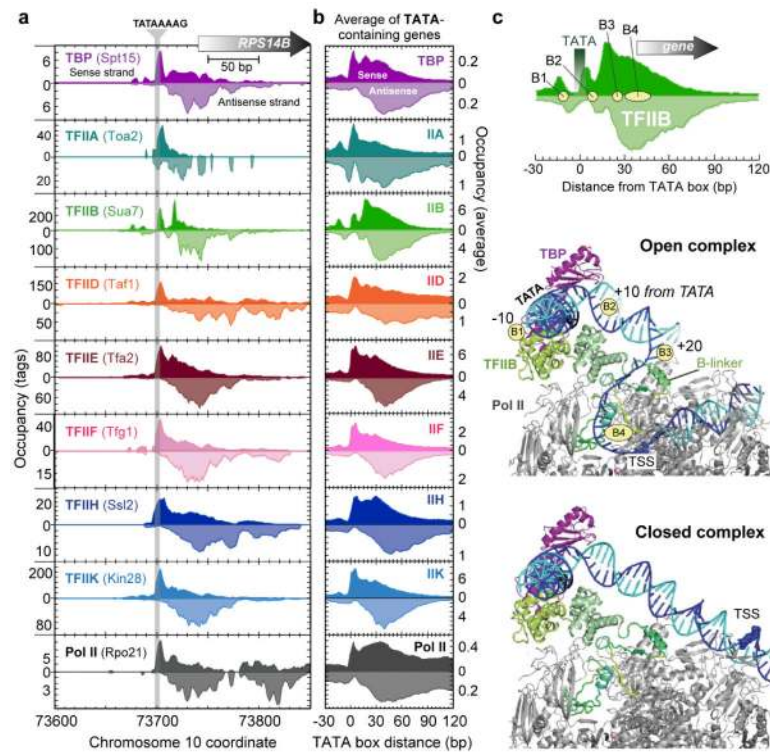


**Figure 1. Genome-wide structural organization of PICs**

**a**, Raw ChIP-exo tag distribution for GTFs and pol II around the *RPS14B* gene. Filled plots represent unfiltered 5' ends of sequencing tags on the sense (darker fill) and antisense strand (lighter fill). **b**, Average GTF and pol II occupancy around the TATA box of 676 annotated mRNA genes. Plots are as in panel a. **c**, Relationship of four TFIIB crosslinking points to crystallographic-based models of the PIC<sup>14</sup>. Upper panel is expanded from panel b for TFIIB. The middle and lower panels show modeled "open" and "closed" TBP/TFIIB/Pol II/promoter DNA complexes, respectively.

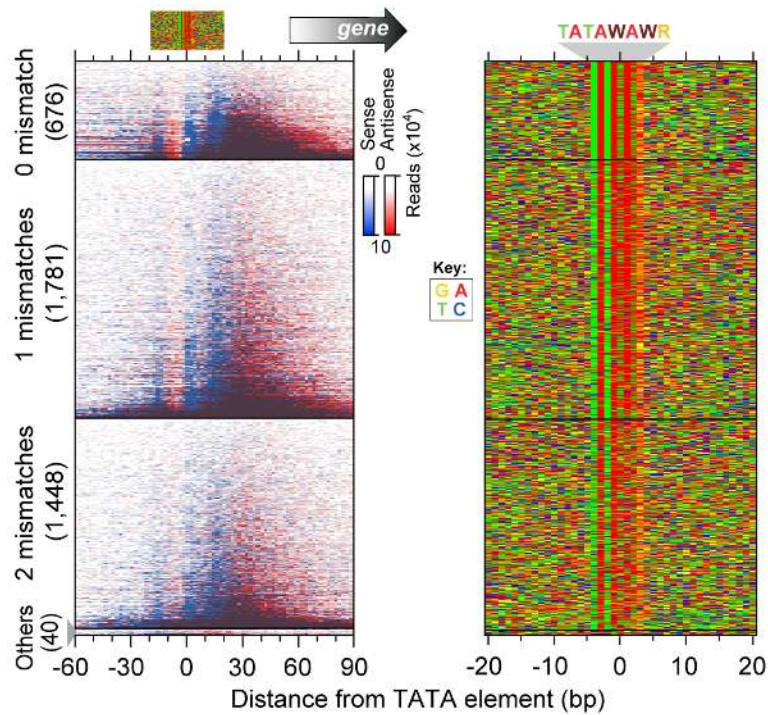


**Figure 2. Identification of TATA-like elements at TATA-less genes**

The left panel shows TFIIIB occupancy around individual TFIIIB-enriched TATA elements of mRNA genes (rows,  $n=3,945$ ), sorted by occupancy level. Occupancy on the sense (blue) and antisense (red) strands is shown with respect to TSS orientation. The right panel shows a color chart representation of the DNA sequence located between  $\pm 20$  bp from the TATA element midpoint and ordered as shown in the left panel.

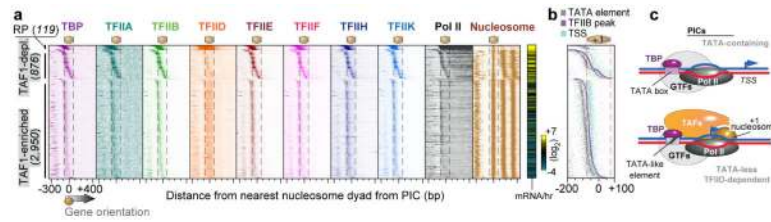


**Figure 3. PIC organization in relation to TFIIID and the +1 nucleosome**

**a.** GTFs occupancy around the nearest nucleosome position (essentially “+1”) to an mRNA PIC, which were sorted by the distance between the two. Unfiltered tags on each strand were shifted in the 3’ direction by a fixed distance (~8 bp depending on each GTF, 73 bp for nucleosomes), so as to better reflect the points of crosslinking. TAF1-depleted and TAF1-enriched genes were determined as being distinct clusters when GTF occupancies of all genes were clustered by k-means (see Fig. 5a). For all graphs of this type, image resolution is less than the number of rows, resulting in some averaging and thus the appearance of less variance across adjacent rows. See Supplementary Data 2 for underlying values, which can be visualized in Treeview. “RP” indicates ribosomal protein genes. The right panel shows transcription frequency<sup>50</sup>. The nucleosome borders are denoted by vertical dashed black lines. **b.** Same as panel a, but showing an overlay of TATA elements, TFIIB, and TSS. **c.** Model of PIC organization at TATA box-containing and TATA-less/TFIID-dependent genes.

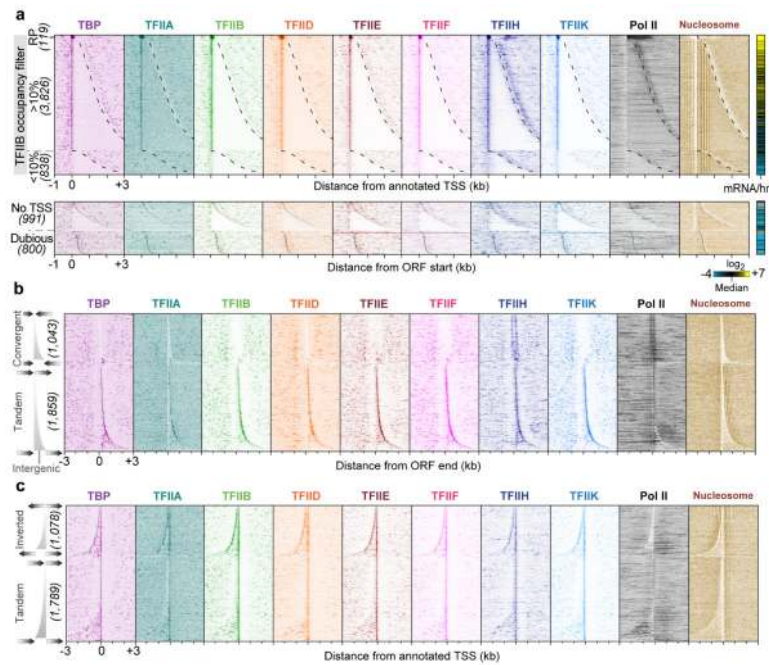


**Figure 4. Genomic view of PICs in relation to genes**

**a**, GTF occupancy around transcript and ORF start sites<sup>49</sup>, sorted by gene length. See Supplementary Data 3-5 for underlying values. Transcript or ORF ends are indicated by black dashed and solid lines, respectively. The right panel shows transcription frequency<sup>50</sup>. **b**, GTF distribution around the 3' ends of mRNA genes, sorted by intergenic length, and sectioned by convergent vs tandem gene-pairs. Occupancy at eight reported looped genes<sup>38,39</sup> is shown in Supplementary Fig. 5. **c**, GTF distribution around the TSS of mRNA genes, sorted by intergenic length, and sectioned by inverted vs tandem gene-pairs.



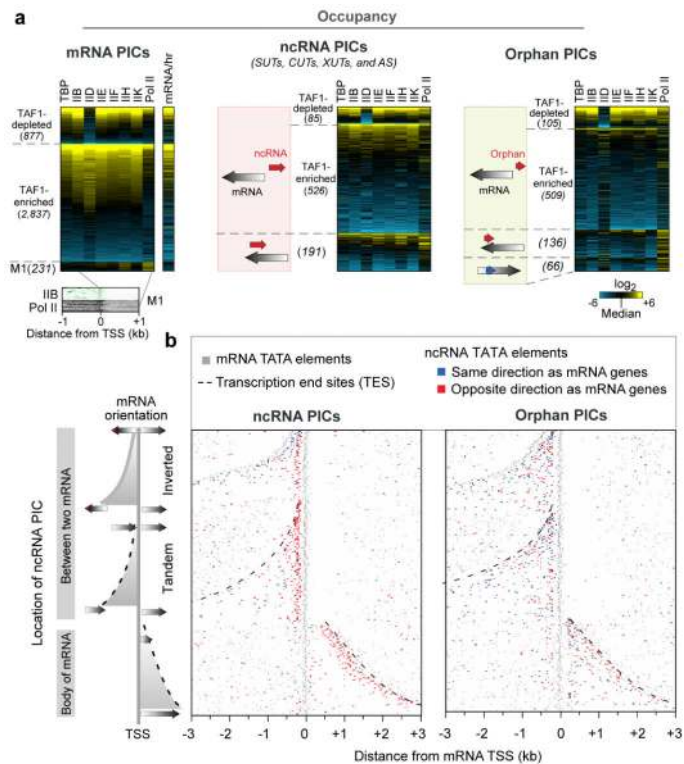


**Figure 5. Distribution of ncRNA PICs**

**a.** GTF occupancy levels at PICs for mRNA, ncRNA, and orphans, sectioned by k-means clustering. Occupancy levels of each GTF were median normalized,  $\log_2$  transformed, then sorted by row median. The small M1 group represents a terminating polymerase originating from upstream. **b.** Distribution of ncRNA PICs relative to mRNA genes. mRNA genes were filtered to retain only those having a nearby ncRNA-associated PIC (defined as having >10% of the genome-wide TFIIB average). Plotted are the locations of TATA elements associated with the mRNA (gray), sense-directed ncRNA (blue), and antisense-directed ncRNA (red). Additional plot details are as described in Fig. 4.